Int. J. Heat Mass Transfer. Vol. 34, No. 12, pp. 3025–3036, 1991
Printed in Great Britain

0017 9310/91 $3.00 + 0.00

An instrumented cylinder for the measurement of instantaneous local heat flux in high temperature fluidized beds

A. H. GEORGE
Department of Mechanical Engineering, Montana State University, Bozeman, MT 59717-0007, U.S.A.

and

J. L. SMALLEY
General Dynamics, Convair Division, San Diego, CA 92123, U.S.A.

(*Received* 18 *July* 1990 *and in final form* 15 *January* 1991)

Abstract—An instrumented cylinder which contains an abrasion resistant, fast responding (settling time of approximately 2 ms) heat flux transducer, along with associated analog signal conditioning equipment, is developed for the measurement of instantaneous local heat transfer rates to an immersed horizontal cylinder in a high temperature fluidized bed. Analog signal conditioning is used to provide a d.c. voltage which is linearly related to the instantaneous local heat flux. This voltage is suitable for direct oscillographic recording or digital data acquisition. Instantaneous local heat transfer coefficient data obtained in a 30×60 cm cross section high temperature fluidized bed of 0.9 mm mean diameter particles at 562°C are presented. Spatially-averaged heat transfer coefficient data, obtained using the instrumented cylinder in fluidized beds with temperatures up to 743°C, are in very good agreement with published correlations.

INTRODUCTION

INSTRUMENTATION for the measurement of instantaneous local heat transfer rates (or, equivalently, instantaneous local heat transfer coefficients) to surfaces immersed in low temperature fluidized beds has been developed and used by several investigators including Mickley *et al.* [1], Gloski *et al.* [2], Tuot and Clift [3], Baskakov *et al.* [4], Fitzgerald *et al.* [5] and Wu *et al.* [6]. These studies also report instantaneous local heat transfer coefficient data for immersed cylinders or immersed plane surfaces in low temperature fluidized beds.

All of the above studies utilized electrically heated foils or thin metal films of low heat capacity as heat flux transducers. The instantaneous electrical power dissipated by the metal film, instantaneous surface temperature, knowledge of the geometry of the transducer and thermal properties of the materials of construction are adequate to calculate the instantaneous local heat flux. The operating principle of these devices and the signal conditioning methods used require that the transducer surface be at a higher temperature than the fluidized bed. For this reason, none of the heat transducers employed in the above studies are useful in high temperature fluidized beds. Abrasion resistance is also limited for devices of this type.

Fluidized bed heat transfer studies that are conducted exclusively at low temperature have several important limitations. The most serious limitation is that the transport properties of the fluidizing gas and particles are essentially fixed and will usually have values greatly different than characteristic of high temperature operation. Radiant heat exchange, which is not negligible in fluidized bed combustors, cannot be studied at low temperatures. Validation of analytical models or empirical data correlations for bed-to-surface heat transfer based exclusively on studies conducted at low temperature is, therefore, not conclusive.

Few measurements of instantaneous local heat transfer rates to surfaces immersed in fluidized beds at elevated temperature have been reported. A heat flux transducer and associated signal conditioning circuit were developed specifically for use in high temperature fluidized beds in ref. [7]. In the aforementioned study, the measuring system was used to obtain instantaneous local bed-to-wall heat transfer coefficients in a fluidized bed of 150 μm diameter glass beads at 282°C. This paper describes a similar heat flux transducer and signal conditioning circuit adapted to the measurement of instantaneous local heat transfer rates on the surface of a 50.8 mm diameter horizontal cylinder. As in the previous work [7], the analog signal conditioning circuit provides a d.c. voltage which is linearly related to the instantaneous local heat flux.

Operating experience with the instrumented cylinder described below includes approximately 70 h of operation in fluidized beds of granular refractory particles with 0.9–2.1 mm mean diameter and temperatures ranging from 548 to 743°C. Local surface

NOMENCLATURE

Ar	Archimedes number
d_p	mean particle size
e	input voltage to signal conditioning circuit
g	acceleration due to gravity
$\bar{h}$	spatial-average heat transfer coefficient
$\bar{h}_{max}$	maximum spatial-average heat transfer coefficient
$h(t)$	instantaneous local heat transfer coefficient
$\langle h \rangle$	time-average local heat transfer coefficient
k	thermal conductivity of transducer material
k_f	thermal conductivity of fluidizing gas at bed temperature
L	effective length of transducer between thermocouples
$\overline{Nu}_{max}$	maximum spatial-average Nusselt number
$q_w(t)$	instantaneous local heat flux
t	time
T_{bed}	bed temperature
T_L	temperature at in-wall thermocouple
T_w	surface temperature
T_{ref}	reference temperature for calibration factor β
$\langle T_w \rangle$	time-average surface temperature
U_o	superficial gas velocity
v	output voltage from signal conditioning circuit
v_4	output voltage of signal amplification circuit.

Greek symbols

β	calibration factor
ρ	density of transducer material
ρ_f	density of fluidizing gas at the bed temperature
ρ_s	density of particle
ν_f	kinematic viscosity of fluidizing gas at the bed temperature
θ	angular position of transducer on cylinder surface.

temperatures on the outside of the cylinder up to 188°C were maintained for several hours. Operation at higher temperatures is certainly feasible.

A data set, including instantaneous local heat transfer coefficients and corresponding time-average values, for a single horizontal cylinder immersed in a 30 × 60 cm cross section fluidized bed of 0.9 mm mean diameter refractory particles at 562°C, is reported. Time-average local heat transfer coefficients for particles of 2.1 mm mean diameter and fluidized bed temperatures up to 743°C are also provided.

The measurement of time-average local heat transfer coefficients does not require a rapidly responding heat flux transducer and is therefore easier to perform than instantaneous measurements. Time-average local heat fluxes (or, equivalently, time-average local heat transfer coefficients) for horizontal tubes immersed in high temperature fluidized beds have been reported by a few investigators [8, 9]. While these data provide useful information concerning the local heat transfer coefficient around the periphery of an immersed tube, no information whatsoever is provided concerning the temporal variation of the local heat transfer coefficient. The more detailed models of the heat transfer process involve the calculation of instantaneous bed-to-surface heat transfer rates from the instantaneous flow field and voidage distribution near the immersed surface. Time-average data are not adequate for validation or improvement of these sophisticated analytical models.

The geometry, i.e. the immersed horizontal cylinder, considered in this work is of importance since many fluidized bed combustors use arrays of immersed horizontal tubes as heat transfer surfaces [10]. The instrumented cylinder, calibration method, and data acquisition technique described below provide data useful for the validation of analytical models of bed-to-surface heat transfer and for direct use in the design of fluidized bed combustion systems.

INSTRUMENTED CYLINDER, HEAT FLUX TRANSDUCER, AND ANALOG SIGNAL CONDITIONING UNIT

Design of instrumented cylinder

The instrumented cylinder, which is water-cooled, allows the positioning of the heat flux transducer in the fluidized bed. For the present application, the 50.8 mm diameter instrumented cylinder was mounted horizontally in packing glands and supplied with coolant (water) through rotary unions. This mounting arrangement allowed the rotation of the cylinder to different angular positions without disconnecting any piping. A single heat flux transducer was used to take data at all angular positions considered.

Figure 1 shows the design of the instrumented cylinder. The instrumented cylinder was constructed of type 304 stainless steel and composed of three pieces: the transducer cover plate, the wire channel cover plate, and the cylinder itself. The cylinder was designed so that the heat flux transducer—described in the next section—would slip into the bored recess shown in cross section B–B, and lightly press fit in the diameter indicated at point D. A small amount of high temperature silicone gasket seal was placed at point E to produce a water tight seal. The transducer

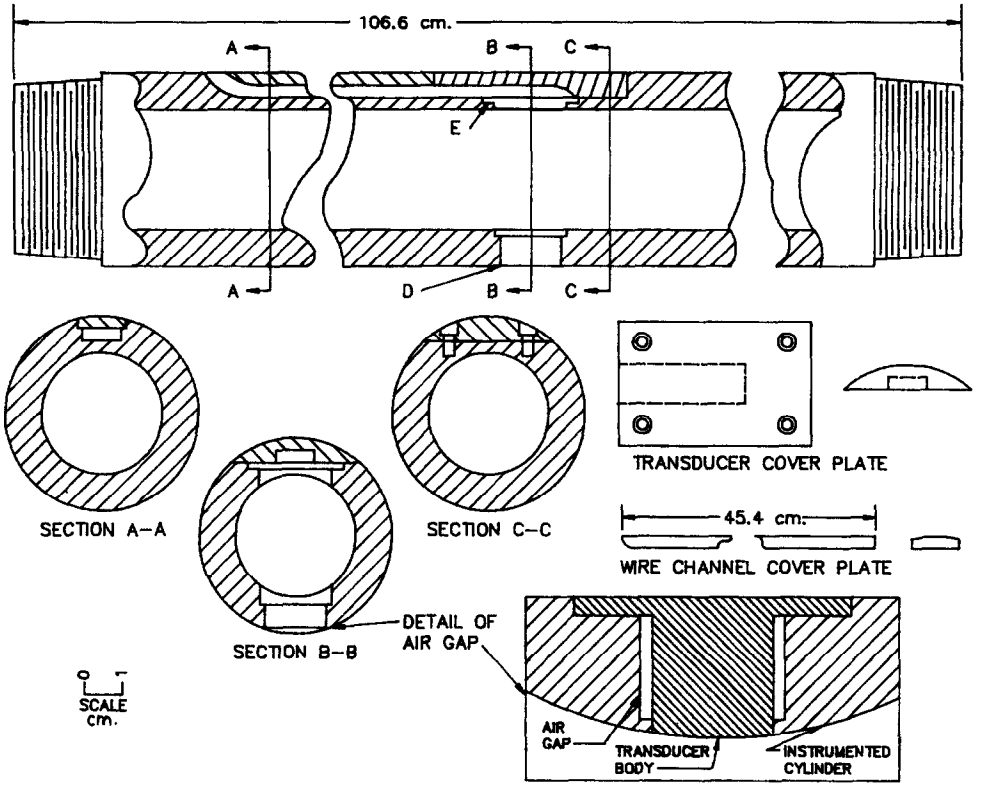

FIG. 1. Instrumented cylinder.

cover plate was fitted over the non-active end of the transducer. The wire channel cover plate was lightly press fitted into the wire channel slot and retained by stainless steel screws. This cover served to protect the wires from the fluidized bed environment. Easy installation and removal of the transducer from the cylinder was provided by this design.

The instrumented cylinder incorporated a 0.25 mm air gap between the cylinder and the clamping ring on the transducer as shown in the detail on Fig. 1. This gap insulated the peripheral surface of the transducer and was intended to help ensure one-dimensional heat transfer within the transducer. Similar transducers used for measuring heat transfer rates in internal combustion engines have successfully used this construction [11, 12].

Design of heat flux transducer

It was shown previously [7] that measurement of the instantaneous surface temperature and the in-wall temperature (about 6 mm from the surface in this design) is required to solve the conduction problem for the transducer body and, subsequently, compute the instantaneous local heat flux at the surface. Therefore, the transducer contains two temperature measuring elements.

The design and principle of operation of the heat flux transducer was based on analysis previously described in ref. [7]. However, several significant changes in internal construction were required for the present application. The heat flux transducer, which was mounted in the instrumented cylinder, is shown in Fig. 2. This heat flux transducer was constructed of type 304 stainless steel and contains an eroding-type thermocouple (also called ribbon thermocouple) which measures the temperature at the surface of the transducer. The eroding-type thermocouple junction consists of two ANSI type K thermocouple wire rib-

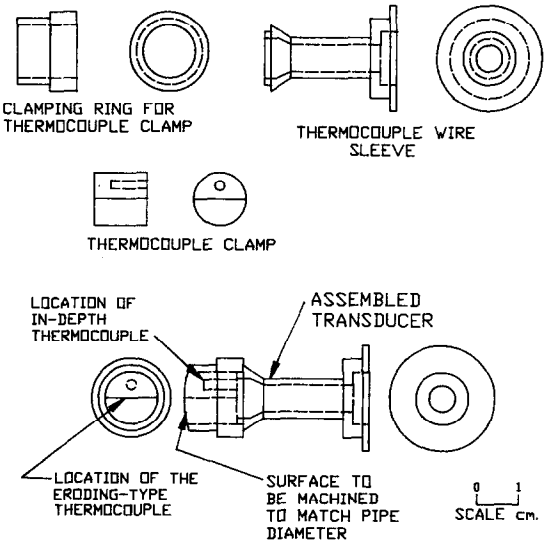

FIG. 2. Heat flux transducer.

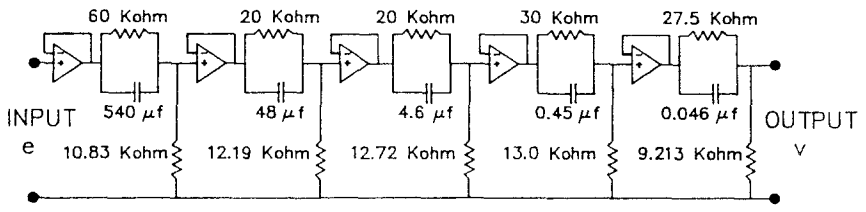

FIG. 3. Analog signal conditioning circuit.

bons that were forged to a thickness of 0.025 mm and pressed between three mica sheets which were used as insulating material, so the wire ribbons were only able to contact each other at the surface of the transducer. The two mica sheets that electrically insulate the thermocouple wire ribbons from the body of the transducer were split to a thickness of 0.025 mm. The remaining mica sheet that electrically insulates the wire ribbons from each other was split to an approximate thickness of 0.012 mm. Small burrs of thermocouple metal at the surface, which bridge over the thin mica sheets, form the actual surface thermocouple junction. These burrs also contact the surface of the transducer body, creating a grounded thermocouple junction of extremely low thermal mass at the surface. The effective width of the eroding-type thermocouple junctions was approximately 5 mm.

A welded junction ANSI type K thermocouple was mounted at an approximate depth of 6 mm from the surface. This in-wall junction was attached to the transducer body with silver solder.

The wire sleeve, which contains the thermocouple wires, was reduced to the smallest allowable outside diameter so that the flow of coolant was not significantly restricted. A detailed description of the techniques used to assemble the heat flux transducer and instrumented cylinder is given in ref. [13].

Signal conditioning circuit

An analog signal conditioning circuit was used to process the voltage output of the eroding-type surface thermocouple. The voltage output of the analog signal conditioning circuit is linearly related to the surface heat flux. The basic design and theory of operation of the circuit was given previously [7]. Operating experience has, however, indicated a definite need to determine the input–output relationship of the combined heat flux transducer and signal conditioning circuit by calibration. Computed input–output relationships based on the thermal properties of the transducer body, sensitivity of the thermocouples, and circuit analysis differed by approximately 35% from those obtained by calibration.

A useful check on the input–output relationship for the analog signal conditioning circuit was to subject the transducer to a step change in the surface heat flux and verify that a near step change in the output voltage was produced. A movie projector with a 750 W lamp and a manual shutter were used as a radiant heat source to produce a step change in heat flux at the transducer surface. Initially the voltage output from the signal conditioning circuit did not yield a near step change, but produced a peak overshoot of approximately 30% that was unacceptable for use in measuring instantaneous changes in the local heat flux to the surface. In order to eliminate the peak overshoot, several of the resistors in the analog circuit were adjusted until the overshoot disappeared. The adjusted analog signal conditioning circuit is shown in Fig. 3. This circuit was then used as part of the signal amplification circuit shown in Fig. 4 that was interfaced directly with a digital data acquisition system. Four-pole Bessel low-pass filters with cut-off frequency (-3 db) of 900 Hz were used with both of the amplifiers shown to improve signal-to-noise ratio.

The input–output relationship for the transducer and signal amplification circuit combined was rechecked by again subjecting the transducer to a step change in surface heat flux. Since a step input contains a wide range of frequencies, an accurate response to a step input verifies both the amplitude response and phase response characteristics of the system. A propane torch and shutter were used to produce a step change in heat flux of short (8 ms) duration at the transducer surface. The output voltage of the signal amplification system (v_4) was recorded on a digital storage oscilloscope. Figure 5 shows the response of the combined transducer and signal amplification circuit to a step change in surface heat flux of approximately 200 kW m^{-2}. The settling time (defined as the time interval after application of a step change in surface heat flux for the output voltage to remain within 2% of the final value), as obtained from Fig. 5, is approximately 2 ms and no significant overshoot is present. Two similar tests were done to check the response of the circuit for a step change in surface heat flux of long duration (approximately 10 and 50 s).

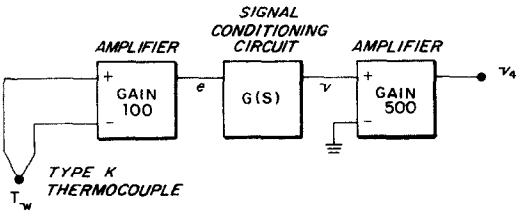

FIG. 4. Signal amplification circuit.

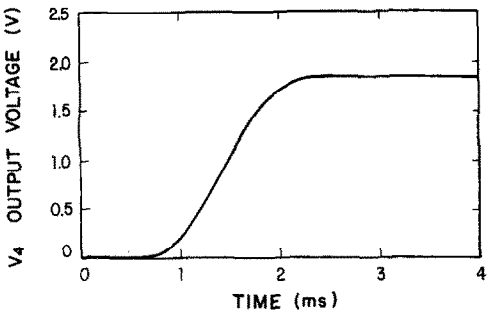

FIG. 5. Response of the combined heat flux transducer and signal amplification circuit to a step change in surface heat flux.

A movie projector with a 750 W lamp was used as a radiant source to produce the step change in surface heat flux and the output voltage (v_4) was recorded on an XY plotter. For values of time greater than the settling time, the output voltage (v_4) was determined to be constant within ± 6 and $\pm 10\%$, respectively, for these tests. Therefore, the overall response characteristics of the combined transducer and signal amplification circuit were satisfactory for the application considered here.

The settling time reported above is shorter than that provided by other systems for heat flux measurement in fluidized beds. For example, Wu *et al.* [6] reported a 90% complete response to a step change in surface heat flux in 45 ms. Assuming approximately first-order response characteristics, this would correspond to a settling time, as defined above, of approximately 76 ms. The instrumentation used by Catipovic *et al.* [14, 15] provided a settling time of approximately 20 ms. Even when compared with instruments suitable only for use in low temperature fluidized beds, the system used in the present study was faster responding by a factor of approximately 10 or 40. Improved resolution of the temporal variations of the instantaneous local heat transfer coefficient is a result of short settling time.

CALIBRATION

The instantaneous local heat flux is represented as the sum of two terms. One term represents the time-average component of the heat flux while the second term represents the instantaneous changes in the heat flux. As shown in ref. [7], the instantaneous local heat flux is computed from

$$q_w(t) = \frac{k}{L}[\langle T_w \rangle - T_L] + \frac{1}{\beta}[v_4(t) - \langle v_4 \rangle]. \quad (1)$$

The corresponding instantaneous local heat transfer coefficient is given by

$$h(t) = \frac{q_w(t)}{T_{bed} - \langle T_w \rangle}. \quad (2)$$

Both (k/L) and β must be established by calibration.

The factor β is the sensitivity of the signal amplification circuit shown in Fig. 4 to changes in heat flux at the transducer surface. Calibration of the heat flux transducer and associated signal conditioning circuit to determine β was conducted using a radiant heat source to produce a step change in the surface heat flux. The radiant heat source used was a movie projector with the shutter removed. The maximum heat flux the projector would provide at the surface of the cylinder was approximately 10 kW m^{-2}.

A commercial heat flux transducer, with known calibration characteristics, was used to determine the magnitude of the step change in heat flux at the surface of the cylinder. The commercial transducer used was a Micro-Foil heat flow sensor model 20455-1 (Rdf Corporation, Hudson, New Hampshire, U.S.A.). The Micro-Foil heat flow sensor was mounted on a portion of the stainless steel instrumented cylinder that was not exposed to the fluidized bed. Both transducers were covered with soot so that the surface absorptivity would be the same for each transducer. A manually controlled metal shutter was placed in front of the projector lens and then opened to produce a step change in heat flux. The step change in heat flux had a duration longer than the settling time of each transducer. The calibration factor β was established by comparing the voltage output (v_4) of the circuit with the heat flux indicated by the Micro-Foil heat flow sensor. This process was initially done at room temperature and then extended to elevated temperatures (up to 107°C) by first heating the cylinder in an oven. A total of 240 data points were obtained in this calibration process.

Since the characteristics of the signal conditioning circuit and signal amplification circuit are constant, β is a function only of the transducer surface temperature T_w. The calibration results were well correlated (within approximately 4%) by equation (3) below where T_w and T_{ref} are in Kelvin. The reference temperature T_{ref} was 25°C (298 K)

$$\beta = 9.46\left(\frac{T_w}{T_{ref}}\right)^{-0.409} \mu V\,m^2\,W^{-1}. \quad (3)$$

Calibration to establish the value of k/L was done in the high temperature fluidized bed. The method used for calibration was again one of comparison. A Micro-Foil heat flow sensor (model 20455-1), previously used by Goshayeshi *et al.* [16], was used as the standard. This heat flow sensor was mounted on a 50.8 mm diameter cylinder made of SAE 660 bronze. The heat flow sensor was covered with a 0.127 mm thick sheet of stainless steel to protect it from the environment of the fluidized bed. Both cylinders were placed in the fluidized bed with centerlines 0.36 m above the distributor plate. The cylinders were placed 0.2 m apart in the fluidized bed so as not to interfere with particle movement between them. The heat flux transducers were positioned facing downward. This angular position was chosen because, according to

refs. [8, 16], the time-average local heat transfer coefficient was least influenced by the changes in superficial gas velocity at this location. It was assumed that the time-average heat transfer coefficient would be the same for both transducers, since the bed temperature was the same and surface temperature was within 20°C for both transducers.

There was a problem with this calibration method related to a defect in the fluidized bed used. The distributor plate which let the hot gas into the bed was warped from repeated high temperature use. Consequently, the bubbles were not distributed uniformly in the bed and both immersed cylinders were not subjected to identical conditions. Therefore, instead of calculating k/L for a variety of surface temperatures, the value of k/L was determined at a single surface temperature. Several test runs were done at a constant surface temperature of 136°C; the value of k/L was calculated to be constant at 1572 W m^{-2} K^{-1}. The use of a single value for k/L does not alter the accuracy of the measured time-average heat transfer rate significantly because the surface temperature changed by less than 55°C from 136°C for all the test runs considered in this article. This 55°C temperature difference corresponds to an approximately 5% change in thermal conductivity (k) of the transducer material. Uncertainty in the value of k/L related to the non-uniform fluidization characteristics of the particular fluidized bed used is difficult to specify but probably greater than the 5% figure mentioned above.

TEST CONDITIONS

Fluidized bed

The fluidized bed was refractory insulated and used a test section with a 0.30×0.60 m cross section. For the tests reported here, the instrumented cylinders—one for establishing the calibration factor k/L and the other for measuring the instantaneous local heat flux—were positioned with centerlines approximately 0.20 m apart in a horizontal plane approximately 0.36 m above the distributor plate. The packed bed height was 0.10 m above the centerlines of the instrumented cylinders.

The distributor plate was made of two 3.2 mm thick Inconel plates. The top plate contains 171 holes 6.35 mm in diameter placed on 31.75 mm centers in a square array pattern. An identical lower plate was used except for having 9.53 mm holes. To prevent particles from flowing back through the distributor plate when the bed was not fluidized, a stainless steel screen with 0.46 mm diameter wire and approximately 50% open area was placed between the plates.

Granular refractory material with commercial designation Ione Grain was used as the bed material (particles). This material had a solids density of 2700 kg m^{-3}.

A positive displacement air blower supplied air to a propane burner and, subsequently, to the fluidized bed. No combustion occurred in the fluidized bed itself. The flow rate of air into the fluidized bed was established using a venturi flowmeter.

Table 1. Fluidized bed conditions for each of the test runs considered

	Run number		
	1	2	3
Bed temperature (°C)	562	548	743
Gas velocity (m s^{-1})	1.0	2.81	2.81
Particle size (mm)	0.9	2.1	2.1
Spatial-average cylinder surface temperature (°C)	152	115	163

The fluidized bed was in operation, at elevated temperature, for approximately 70 h. During that time three test runs were completed. Table 1 shows the operating conditions for the three test runs. Each test run consisted of instantaneous surface heat flux measurements being recorded at five angular positions around the cylinder. The angular positions of the transducer at which data were recorded are shown in Fig. 6.

Test procedure

The fluidized bed was allowed to reach steady state operating conditions at the selected temperature and superficial gas velocity. A data acquisition system (Hewlett Packard HP3054A with 3456 and 3437 voltmeters) was then used to take 100 s of instantaneous surface heat flux measurements, with a sampling interval of 5 ms, for each of the five angular positions. The sampling interval used was the shortest the data acquisition system would provide. However, a shorter sampling interval (approximately 1 ms) would be more consistent with the settling time of the heat flux transducer used.

The first set of data was taken at $\theta = 0°$; then the cylinder was rotated 45° and the next data set was recorded. This procedure was continued until data were taken at all five angular positions. The voltages required to compute the local time-average surface temperature and in-wall temperature were also recorded by the data acquisition system. The bed tem-

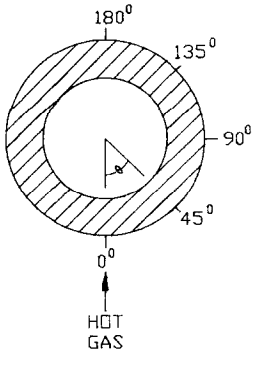

FIG. 6. Angular positions at which instantaneous local heat flux measurements were made.

perature was maintained within $\pm 5°C$ of the specified value for all three test cases considered.

TEST RESULTS

Figures 7–9 show 4 s of typical instantaneous local heat transfer coefficient values for three angular positions at a bed temperature of 562°C (run number 1). This data set was selected for presentation since it used a particle size (0.9 mm mean diameter) similar to that normally employed in fluidized bed combustion of solid fuels such as coal. The electrical noise level, whose source is primarily the signal amplification circuit, corresponds to a heat transfer coefficient fluctuation of approximately ± 22 W m^{-2} K^{-1}.

Several interesting observations can be made from inspection of this data set. First, Figs. 7 and 8 display time intervals with relatively constant but low heat transfer coefficient, e.g. the time interval from 3.7 to 3.8 s on Fig. 7. These are interpreted to be periods of local bubble phase contact with the surface of the cylinder. Figure 9, which corresponds to the angular position 180°, shows no periods of local bubble phase contact. A stack of defluidized particles, which is moved by passing bubbles, normally covers this portion of an immersed horizontal cylinder [17–19]. Therefore, it is quite reasonable that pure bubble phase contact is seldom observed at these angular positions near the top of an immersed horizontal cylinder.

The noise level of approximately ± 22 W m^{-2} K^{-1}

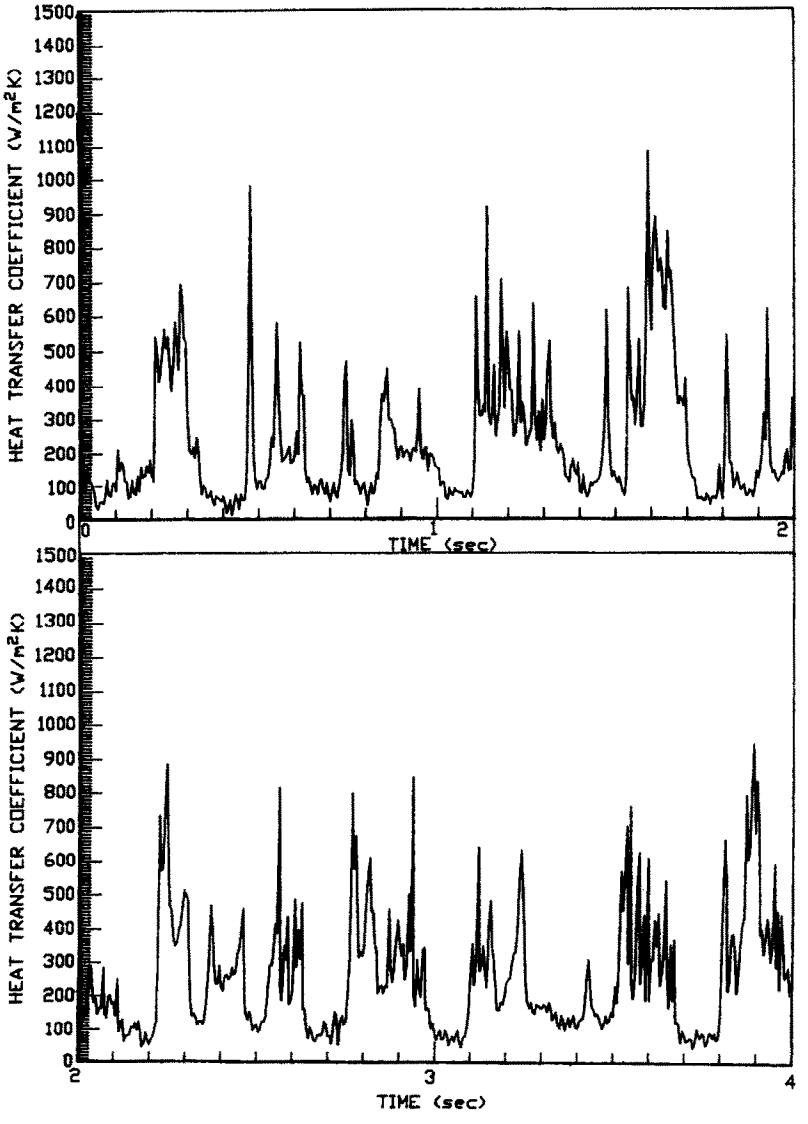

FIG. 7. Instantaneous local heat transfer coefficient for $d_p = 0.9$ mm, $\theta = 0°$, $U_o = 1$ m s^{-1}, $T_{bed} = 562°C$ (run number 1).

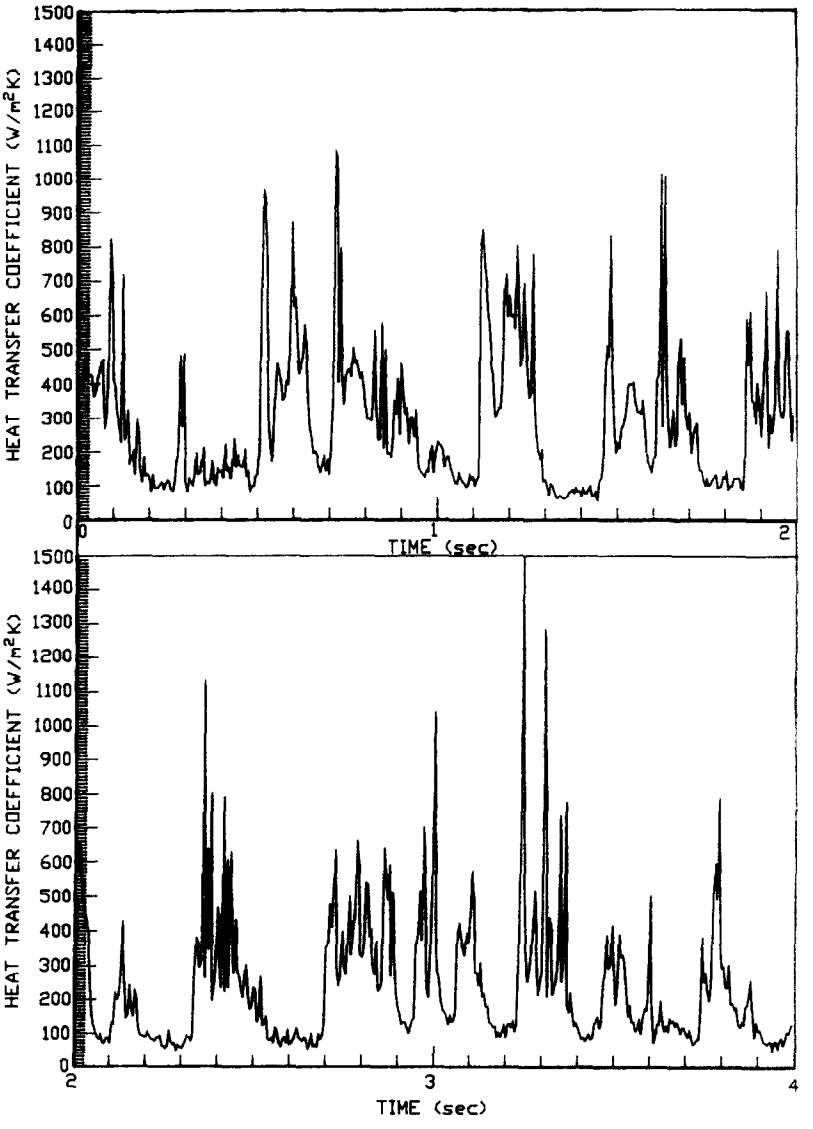

FIG. 8. Instantaneous local heat transfer coefficient for $d_p = 0.9$ mm, $\theta = 45°$, $U_0 = 1$ m s^{-1}, $T_{bed} = 562$ C (run number 1).

is the minimum fluctuation which is possible in the measured instantaneous local heat transfer coefficient. This minimum fluctuation is observed in Fig. 9 during the time interval 0–0.15 s. The fluctuations in the instantaneous local heat transfer coefficient during periods of local bubble phase contact are usually of larger amplitude than could be attributed to the electrical noise level in the measurement system. Conversely, the fluctuations in the instantaneous local heat transfer coefficient during periods of local bubble phase contact are much smaller than those present during local emulsion phase contact (discussed below). It is, therefore, improbable that the observed fluctuations during local bubble phase contact are due entirely to particle contact with the surface thermocouple. A possible explanation is that turbulent flow exists either in the boundary layer or free stream during periods of bubble phase contact.

During periods of local emulsion phase contact, it is observed that instantaneous local heat flux fluctuations are usually at a frequency much higher than the mean bubble frequency. For example, see the time interval 3.25–3.4 on Fig. 8. The high frequency fluctuations which occur during periods of emulsion phase contact could be due to packets of particles and gas which slide over the surface due to nearby bubble movement. Therefore, the surface thermocouple junction is alternatively subjected to particle contact and contact with the gas in the interstitial channels between particles. The observed high frequency fluctuations imply that the local instantaneous heat transfer coefficient varies strongly on a small spatial scale

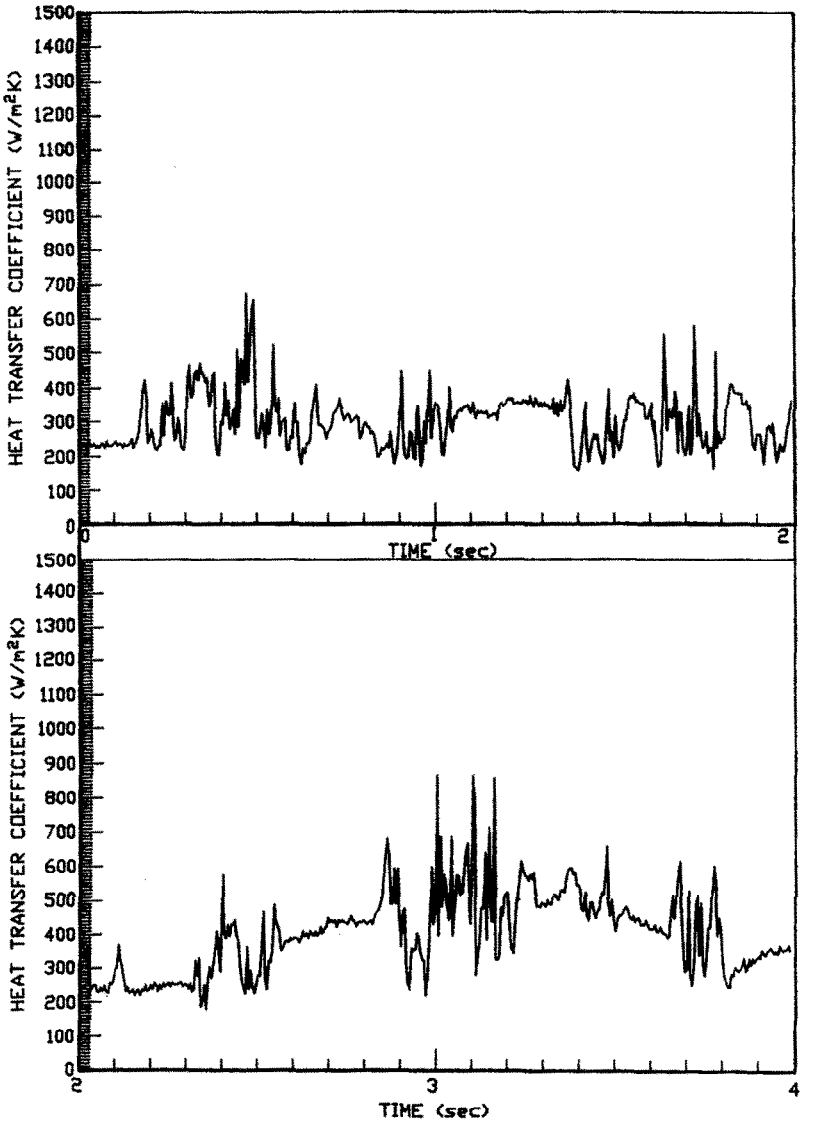

FIG. 9. Instantaneous local heat transfer coefficient for $d_p = 0.9$ mm, $\theta = 180°$, $U_o = 1$ m s^{-1}, $T_{bed} = 562°C$ (run number 1).

(of the order of one particle diameter). The mean frequency of local bubble contact with the cylinder at the angular location $\theta = 45°$ was 2 Hz as established by inspection of the measured instantaneous local heat transfer coefficient.

No instantaneous local heat transfer coefficient data for the operating conditions considered here have been reported elsewhere. Therefore, the instantaneous local heat transfer coefficient data obtained during this study cannot, at this time, be compared directly with data obtained by other investigators.

Tables 2–4 show the time-average local heat transfer coefficient, time-average local surface temperature and spatial-average heat transfer coefficient for each of the three run conditions. The spatial-average heat transfer coefficient was computed from the corresponding local values by application of the trapezoidal rule for numerical quadrature. For all three run conditions, the time-average local heat transfer coefficient was largest at the top of the cylinder ($\theta = 180°$). For given run conditions, the local surface temperature increased as the corresponding time-average local heat transfer coefficient increased.

Data shown in Tables 3 and 4 are for conditions similar to those in an earlier study [8] which was conducted in the same fluidized bed but utilized a different method of measuring the time-average local heat transfer coefficient. The previous study [8] used lower maximum superficial gas velocities (2.4 m s^{-1} rather than 2.81 m s^{-1}) and yielded time-average local

Table 2. Local surface temperature, time-average local heat transfer coefficient and spatial-average heat transfer coefficient for $T_{bed} = 562°C$, $d_p = 0.9$ mm, $U_o = 1$ m s^{-1} (run number 1)

θ (deg)	$\langle T_w \rangle$ (°C)	$\langle h \rangle$ (W m^{-2} K^{-1})
0	127	247
45	131	262
90	153	324
135	175	384
180	174	384
		$\bar{h} = 321$

Table 3. Local surface temperature, time-average local heat transfer coefficient and spatial-average heat transfer coefficient for $T_{bed} = 548°C$, $d_p = 2.1$ mm, $U_o = 2.81$ m s^{-1} (run number 2)

θ (deg)	$\langle T_w \rangle$ (°C)	$\langle h \rangle$ (W m^{-2} K^{-1})
0	93	155
45	97	167
90	119	231
135	129	248
180	138	272
		$\bar{h} = 215$

Table 4. Local surface temperature, time-average local heat transfer coefficient and spatial-average heat transfer coefficient for $T_{bed} = 743°C$, $d_p = 2.1$ mm, $U_o = 2.81$ m s^{-1} (run number 3)

θ (deg)	$\langle T_w \rangle$ (°C)	$\langle h \rangle$ (W m^{-2} K^{-1})
0	136	175
45	143	191
90	167	241
135	182	260
180	188	274
		$\bar{h} = 229$

heat transfer coefficients approximately 14–29% lower than the present study. The largest differences occurred at the top of the cylinder ($\theta = 180°$) which is also the angular position at which the time-average local heat transfer coefficient is most strongly influenced by changes in superficial gas velocity [8, 16]. No time-average local heat transfer coefficient data comparable to those shown in Table 2 have been reported elsewhere.

Superficial gas velocities considered in the work reported here were selected to provide a near maximum spatial-average heat transfer coefficient. The maximum spatial-average Nusselt number and Archimedes number were computed for each of the three run conditions using the following equations:

$$\overline{Nu}_{max} = \frac{d_p \bar{h}_{max}}{k_f} \tag{4}$$

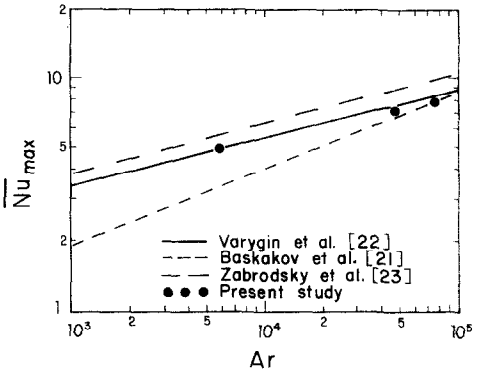

FIG. 10. Maximum spatial-average Nusselt number vs Archimedes number.

$$Ar = \frac{g d_p^3 (\rho_s - \rho_f)}{\rho_f \nu_f^2}. \tag{5}$$

Correlations of the maximum spatial-average Nusselt number as a function of the Archimedes number have been developed by several investigators [20]. Specific correlations valid for the Archimedes number range considered here were developed by Baskakov *et al.* [21], Varygin and Martyushin [22], and Zabrodsky *et al.* [23]. Almost all of the data correlated by these investigators were obtained at near room temperature with air as the fluidizing gas. All gas properties were evaluated at the corresponding bed temperature. These correlations are compared with results of the present study in Fig. 10. The experimental data reported here are well within the range predicted by the three correlations.

CONCLUSIONS

The heat flux transducer and associated analog signal conditioning circuit described in ref. [7] has proven to be adaptable to the measurement of instantaneous local heat transfer coefficients on the surface of a 50.8 mm diameter instrumented cylinder immersed in a high temperature fluidized bed. Fluidized bed temperatures up to 743°C and transducer surface temperatures up to 188°C were successfully used. Operation of the instrumented cylinder in a fluidized bed at combustion level temperatures (approximately 850°C) is certainly feasible.

Abrasion resistance of the heat flux transducer appears to be adequate for most research uses. Approximately 70 h of operation in a high temperature fluidized bed with mean particle sizes as large as 2.1 mm were successfully completed with no failures of the eroding-type surface thermocouple junction and no detectable change in calibration.

The analog signal conditioning circuit reported in ref. [7] required adjustment, i.e. change in some of the resistance values, in order to provide useful response characteristics in the application considered here. After this adjustment, the system provided an experimentally measured settling time (time interval fol-

lowing the application of a step change in surface heat flux for the voltage output to remain within 2% of its final value) of approximately 2 ms and no measurable overshoot. This value of the settling time is significantly shorter than provided by most systems previously used in low temperature fluidized beds. Improved resolution of the temporal variations in the instantaneous local heat transfer coefficient is a result of this short settling time. Each transducer built will require slightly different adjustment of the analog signal conditioning circuit in order to achieve optimal response characteristics (short settling time and absence of overshoot).

The calibration factors β and k/L, which are required to compute the instantaneous local heat flux, can be obtained using commercially available heat flux transducers (Micro-Foil heat flow sensors, RdF Corporation, Hudson, New Hampshire, U.S.A.) as reference transducers. In the present application, a radiant heat source was used to establish β for a range of surface temperatures. The calibration factor k/L was established *in situ* during operation of the instrumented cylinder in the high temperature fluidized bed.

Measurements of the instantaneous local heat transfer coefficient, made using the instrumented cylinder described in this paper, show distinct time intervals during which local bubble phase contact occurs. The lower portion of the immersed horizontal cylinder (angular positions 0°, 45° and 90°) is contacted by bubbles much more often than the upper portion (angular positions 135° and 180°).

High frequency (much greater than the mean bubble frequency) fluctuations in the instantaneous local heat transfer coefficient occur during periods of local emulsion phase contact. Sliding of the particle/gas emulsion over the heat flux transducer is the suggested cause of this phenomena. The eroding-type surface temperature thermocouple junction is exposed to alternate contact with particles and gas in the interstitial channels between particles during periods of emulsion phase contact.

Values of the spatial-average heat transfer coefficient obtained during the present study are in very good agreement with established correlations. Comparable time-average local heat transfer coefficient data, obtained by an alternate measurement technique, show good agreement (within 29%) with the corresponding values reported above.

Acknowledgements—The authors wish to thank Mr Pat Vowell for fabricating the instrumented cylinder described above and Mr John Rompel for building the associated analog signal conditioning circuit and signal amplification circuit. This work was supported, in part, by the National Science Foundation (grant number CBT-8801618).

REFERENCES

1. H. S. Mickley, D. F. Fairbanks and R. D. Hawthorn, The relation between the transfer coefficient and thermal fluctuations in fluidized-bed heat transfer, *Chem. Engng Prog. Symp. Ser.* **57**(32), 51–60 (1961).
2. D. Gloski, L. Glicksman and N. Decker, Thermal resistance at a surface in contact with fluidized bed particles, *Int. J. Heat Mass Transfer* **27**, 599–610 (1984).
3. J. Tuot and R. Clift, Heat transfer around single bubbles in a two-dimensional fluidized bed, *A.I.Ch.E. Symp. Ser.* **69**(128), 78–84 (1973).
4. A. P. Baskakov, O. K. Vitt, V. A. Kirakosyan, V. K. Maskayev and N. F. Filippovsky, Investigation of heat transfer coefficient pulsations and of the mechanism of heat transfer from a surface immersed into a fluidized bed. In *La Fluidisation et Ses Applications—Congress International*, Vol. 1. Cepadues, Toulouse, France, 1–5 October (1973).
5. T. J. Fitzgerald, N. M. Catipovic and G. N. Jovanovic, Instrumented cylinder for studying heat transfer to immersed tubes in fluidized beds, *Ind. Engng Chem. Fundam.* **20**, 82–88 (1981).
6. R. L. Wu, C. J. Liu and J. R. Grace. The measurement of instantaneous local heat transfer coefficients in a circulating fluidized bed, *Can. J. Chem. Engng* **67**, 301–307 (1989).
7. A. H. George, A transducer for the measurement of instantaneous local heat flux to surfaces immersed in high temperature fluidized beds, *Int. J. Heat Mass Transfer* **30**, 763–769 (1987).
8. A. H. George and J. R. Welty, Local heat transfer coefficients for a horizontal tube in a large-particle fluidized bed at elevated temperature, *A.I.Ch.E. Jl* **30**, 482–485 (1984).
9. A. Goshayeshi, J. R. Welty, R. L. Adams and N. Alavizadeh, An experimental study of heat transfer in an array of horizontal tubes in large particle fluidized beds at elevated temperatures, 23rd ASME/AIChE Natn. Heat Transfer Conf., Denver, Colorado, U.S.A., 4–7 August (1985).
10. J. Makansi and R. Schwieger, Fluidized bed boilers, *Power* **131**, S1–S15 (1987).
11. A. C. Alkidas and R. M. Cole, Transient heat flux measurements in a divided-chamber diesel engine, *ASME J. Heat Transfer* **107**, 439–445 (1985).
12. A. C. Alkidas and J. P. Myers, Transient heat flux measurements in the combustion chamber of a spark-ignition engine, *ASME J. Heat Transfer* **104**, 62–67 (1982).
13. J. L. Smalley, Development of a transducer to measure instantaneous local heat flux to a surface immersed in a high temperature fluidized bed, M.S. Thesis, Montana State University, Bozeman, Montana, U.S.A. (1990).
14. N. M. Catipovic, T. J. Fitzgerald and G. Jovanovic, A study of heat transfer to immersed tubes in fluidized beds, Paper 28e, A.I.Ch.E. 71st Annual Meeting, Miami, Florida, U.S.A., 12–16 November (1978).
15. N. M. Catipovic, T. J. Fitzgerald, A. H. George and J. R. Welty, Experimental validation of the Adams–Welty model for heat transfer in large-particle fluidized beds, *A.I.Ch.E. Jl* **28**, 714–720 (1982).
16. A. Goshayeshi, J. R. Welty, R. L. Adams and N. Alvizadeh, An experimental study of heat transfer in an array of horizontal tubes in large particle fluidized beds at elevated temperatures, 23rd ASME/AIChE Natn. Heat Transfer Conf., Denver, Colorado, U.S.A., 4–7 August (1985).
17. D. H. Glass and D. Harrison, Flow patterns near a solid obstacle in a fluidized bed, *Chem. Engng Sci.* **19**, 1001–1002 (1969).
18. O. Loew, B. Schmutter and W. Resnick, Particle and bubble behavior and velocities in a large particle fluidized bed with immersed obstacles, *Powder Technol.* **22**, 45–48 (1979).
19. W. R. Hager and S. D. Schrag, Particle circulation downstream from a tube immersed in a fluidized bed, *Chem. Engng Sci.* **31**, 657–659 (1976).
20. N. S. Grewal and J. C. Saxena, Maximum heat transfer coefficient between a horizontal tube and a gas–solid

fluidized bed, *Ind. Engng Chem. Process Des. Dev.* **20**, 108–116 (1981).
21. A. P. Baskakov, B. V. Berg, O. K. Vitt, N. F. Filippovsky, V. A. Kirakosyan, J. M. Goldobin and V. K. Majkaev, Heat transfer to objects immersed in fluidized beds, *Powder Technol.* **8**, 273–282 (1973).
22. N. N. Varygin and I. G. Martyushin, *Khim. Mash.* (1966) (as cited in ref. [20]).
23. S. S. Zabrodsky, N. V. Antonishin, G. M. Vasiliev and A. L. Paranas, *Visti Akad. Nauk BSSR, Ser. Fix-Energ. Nauk* No. 4, 103 (1974) (as cited in ref. [20]).

UN CYLINDRE INSTRUMENTE POUR LA MESURE DU FLUX THERMIQUE LOCAL INSTANTANE DANS DES LITS FLUIDISES A HAUTE TEMPERATURE

Résumé—On développe pour la mesure du transfert local instantané à un cylindre horizontal immergé dans un lit fluidisé à haute température, un cylindre instrumenté qui contient un transducteur thermique, résistant à l'abrasion, à réponse rapide (constante de temps de 2 ms environ), associé à un équipement de signal analogique. Celui-ci est utilisé pour fournir une tension de courant continu qui est linéairement liée au flux thermique local instantané. Cette tension convient à l'observation directe oscillographique ou à l'acquisition sur ordinateur. Le coefficient local de transfert thermique instantané est obtenu dans une section droite 30×60 cm d'un lit fluidisé à haute température de particules de diamètre 0,9 mm en moyenne et à 562°C. Les données de coefficient de transfert moyen spatialement, obtenues avec le cylindre instrumenté dans des lits fluidisés à des températures jusqu'à 743°C, sont en très bon accord avec les formules déjà publiées.

MESSUNG DER MOMENTANEN ÖRTLICHEN WÄRMESTROMDICHTE IN EINEM HOCHTEMPERATUR-WIRBELBETT MIT EINEM INSTRUMENTIERTEN ZYLINDER

Zusammenfassung—Für die Messung der momentanen örtlichen Wärmestromdichte an der Oberfläche eines waagerechten Zylinders in einem Hochtemperatur-Wirbelbett wurde ein Meßgerät entwickelt. Dieses besteht aus einem instrumentierten Zylinder, der einen verschleißfesten, schnell ansprechenden (ungefähre Ansprechzeit 2 ms) Umformer für die Wärmestromdichte, sowie Einrichtungen für die Verarbeitung der entsprechenden Analogsignale enthält. Diese Analogsignalverarbeitung liefert eine Gleichspannung, die linear mit der momentanen örtlichen Wärmestromdichte zusammenhängt. Diese Ausgangsspannung kann nun unmittelbar einem Speicheroszillographen oder einer digitalen Datenverarbeitung zugeführt werden. In einem Hochtemperatur-Wirbelbett mit einem Querschnitt von 30×60 cm und einem mittleren Partikeldurchmesser von 0,9 mm bei 562°C werden momentane örtliche Wärmeübergangskoeffizienten gemessen und dargestellt. Volumengemittelte Wärmeübergangskoeffizienten, die mit Hilfe des instrumentierten Zylinders in einem Wirbelbett bei Temperaturen bis zu 743°C ermittelt worden sind, stimmen gut mit veröffentlichten Korrelationen überein.

ЦИЛИНДР, ОСНАЩЕННЫЙ ПРИБОРАМИ ДЛЯ ИЗМЕРЕНИЯ МГНОВЕННЫХ ЗНАЧЕНИЙ ЛОКАЛЬНОЙ ПЛОТНОСТИ ТЕПЛОВОГО ПОТОКА В ВЫСОКОТЕМПЕРАТУРНЫХ ПСЕВДООЖИЖЕННЫХ СЛОЯХ

Аннотация—Разработан цилиндр, оснащенный стойким к абразивному износу быстродействующим (время установления составляет около 2 мс) датчиком теплового потока и аналоговым устройством по обработке сигналов, который предназначен для измерения мгновенных значений локальной интенсивности теплопереноса к горизонтальному цилиндру, погруженному в высокотемпературный псевдоожиженный слой. Аналоговая обработка сигналов позволяет поддерживать постоянное напряжение, линейно связанное с мгновенным значением локальной плотности теплового потока. При таком напряжении можно производить прямую осциллографическую запись или сбор цифровых данных. Даны значения коэффициента мгновенного локального теплопереноса, полученные при 562°C для псевдоожиженного слоя частиц со средним диаметром, равным 0,9 мм, поперечное сечение которого составляет 30×60 см. Пространственно-осредненные данные по коэффициенту теплопереноса, полученные с использованием разработанного цилиндра в псевдоожиженных слоях при температурах вплоть до 743°C, очень хорошо согласуются с имеющимися в литературе обобщающими соотношениями.